Universal fine-structure eraser for quantum dots

Fognini, A.; Ahmadi, A.; Daley, S. J.; Reimer, M. E.; Zwiller, V.

DOI
10.1364/OE.26.024487

Publication date
2018

Document Version
Final published version

Published in
Optics Express

Research Article | Vol. 26, No. 19 | 17 Sep 2018 | OPTICS EXPRESS 24487
Optics EXPRESS

Universal fine-structure eraser for quantum dots

A. Fognini,[1,*] A. Ahmadi,[2] S. J. Daley,[3] M. E. Reimer,[3] and V. Zwiller[1,4]

[1] *Kavli Institute of Nanoscience Delft, Delft University of Technology, 2628 CJ Delft, The Netherlands*
[2] *Institute for Quantum Computing and Department of Physics & Astronomy, University of Waterloo, Waterloo, ON N2L 3G1, Canada*
[3] *Institute for Quantum Computing and Department of Electrical & Computer Engineering, University of Waterloo, Waterloo, ON N2L 3G1, Canada*
[4] *Department of Applied Physics, Royal Institute of Technology (KTH), AlbaNova University Center, SE - 106 91 Stockholm, Sweden*
[*] *a.w.fognini@tudelft.nl*

Abstract: We analyze the degree of entanglement measurable from a quantum dot via the biexciton-exciton cascade as a function of the exciton fine-structure splitting and the detection time resolution. We show that the time-energy uncertainty relation provides means to measure a high entanglement even in presence of a finite fine-structure splitting when a detection system with high temporal resolution is employed. Still, in many applications it would be beneficial if the fine-structure splitting could be compensated to zero. To solve this problem, we propose an all-optical approach with rotating waveplates to erase this fine-structure splitting completely which should allow obtaining a high degree of entanglement with near-unity efficiency. Our optical approach is possible with current technology and is also compatible with any quantum dot showing fine-structure splitting. This bears the advantage that for example the fine-structure splitting of quantum dots in nanowires and micropillars can be directly compensated without the need for further sample processing.

1. Introduction

Semiconductor quantum dots (QDs) allow for the generation of polarization entangled photons [1–3] through the biexciton-exciton cascade [4]. Effects such as QD shape elongation [5, 6], piezoelectric fields [5], inhomogeneous alloy composition [6, 7], strain fields [8], or more generally all effects lowering the symmetry of the exciton's trapping potential [6] lead to a splitting of the exciton state. The spin-degeneracy of the bright exciton level is therefore normally split in QDs due to the spin-orbit interaction [9]. This splitting is called the fine-structure splitting (FSS) and its energy scale typically lies between $0 - 100\,\mu$eV in the case of III-V semiconductor quantum dots [7, 10]. The FSS introduces a which-path information during the biexciton-exciton decay but only in the limit of slow photon detection. Yet, it was argued as being one of the main reasons for lowering the polarization entanglement [11, 12]. QD growth methods have been successfully developed to minimize the FSS [13–15], but reaching vanishing FSS remains a significant challenge. Consequently, several post-growth techniques have been developed to solve this problem by tuning the FSS to zero. Compensation has been achieved through external strain fields [8,16], magnetic fields [12], electric fields [17,18], annealing [19], or a combination of these approaches [20]. Typically, these techniques act macroscopically on the sample and only fully compensate *one* out of millions of QDs. Scaling up to many quantum dots on the same sample is a challenge. Furthermore, the well established strain compensation technique [8, 16] is difficult to adapt for QDs embedded in photonic nanostructures [7, 15, 21–23] due to strain relaxation over a length scale of $\approx 100\,$nm [22]. Quantum dots embedded in nanowires [7, 15, 22–24] and micropillar cavities [21, 25–28], however, possess several benefits [29] such as enhanced photon extraction due to directional emission and near-unity single mode fiber coupling [30, 31].

#335864 https://doi.org/10.1364/OE.26.024487
Journal © 2018 Received 2 Jul 2018; revised 13 Aug 2018; accepted 13 Aug 2018; published 5 Sep 2018

Optics EXPRESS

Therefore, a universal FSS compensation technique easily applicable to QDs would be of great value.

2. Objective

In this paper, we introduce a novel FSS universal eraser technique which solves above problems and enhances the measurable entanglement towards unity by using frequency shifting capabilities of rotating $\lambda/2$-waveplates applied to both X and XX photons. Of particular significance, this frequency conversion process occurs without loss of photons due to only unitary optical manipulations. FSS compensation techniques [32–36] have been proposed but our approach differs from the one proposed by Wang et al. [32] as it can be implemented with current technology, does not need a large electrical bandwidth to approximate a linear voltage ramp, is not intrinsically slow (≈ 10 kHz) due to high voltage sweeps, and does not rely on the splitting of different polarization modes [33]. Furthermore, we are not suffering from photon loss and can compensate an arbitrarily small FSS in contrast to the scheme proposed by Coish et al. [34]. The reason is that we are not relying on stochastic sideband scattering [35] and don't need an additional filter system to select the right scattered lines preventing compensation in case the FSS is comparable with the QD linewidth. In addition, our approach differs from the phase compensation technique outlined by Zhou et al. [36] as our approach allows to reach unity fidelity regardless of the FSS value, whereas with the phase compensation technique the fidelity can only be enhanced but cannot be brought to unity with a finite FSS.
We start our analysis by discussing the influence of the detection system's time resolution on the measurable entanglement.

3. The influence of time resolution on entanglement

The term detection system includes every component used to detect the arrival time of the two photons from the cascade, e.g., detector time jitter, the electronics to correlate the arrival times of the biexciton and exciton photons, and dispersion in optical components. We define the full width at half maximum of the correlation time distribution of such a system as the time resolution τ. For the sake of clarity we only consider FSS for reducing the measurable entanglement by phase averaging and do not consider dephasing mechanisms [37]. Figure 1(a) depicts the biexciton-exciton cascade without FSS. The cascade starts by the radiative decay of the biexciton (XX) state. Either a right- or left polarized *single* photon is emitted ($|R\rangle$, $|L\rangle$) [5]. After the emission of the XX photon the system is in the exciton state (X). This level is degenerate and $|\uparrow\Downarrow\rangle$, $|\downarrow\Uparrow\rangle$ are the state's eigenfunctions in spin space [5]. Here, $\uparrow, \downarrow$ and $\Uparrow, \Downarrow$ denote the electron and hole spins, respectively. Since we assumed zero FSS, it is impossible to know whether a spin up or down electron has recombined. This lack of knowledge entangles the photons to $|\Phi\rangle = \frac{1}{\sqrt{2}}(|RL\rangle + |LR\rangle)$. In this situation, the detection system's time resolution does not affect the measurable entanglement of this state since it does not change over time. The situation is quite different in the case of finite FSS, as illustrated in Fig. 1(b). Due to spin-orbit interaction the exciton states mix and the new eigenfunctions become $\frac{1}{\sqrt{2}}(|\downarrow\Uparrow\rangle - |\uparrow\Downarrow\rangle)$ and $\frac{1}{\sqrt{2}}(|\downarrow\Uparrow\rangle + |\uparrow\Downarrow\rangle)$ [38]. After the XX decay the X will precess between these two eigenfunctions until it also decays. This evolution makes the quantum state time dependent [39] and reads as

$$|\Psi(t,\delta)\rangle = \frac{1}{\sqrt{2}}\left(|HH\rangle + e^{-t\frac{\delta}{\hbar}t}\,|VV\rangle\right), \tag{1}$$

where δ is the FSS energy, and $|H\rangle$ and $|V\rangle$ denote horizontally and vertically polarized single photon states. Equation (1) describes a fully entangled state even with finite FSS as shown by Stevenson et al. [39]. In fact, a slow detection system ($\tau \gg \hbar/\delta$) will average out the exponential phase term [39] in Eq. (1) and only classical correlations are detected [40]. In contrast, a fast

Optics EXPRESS

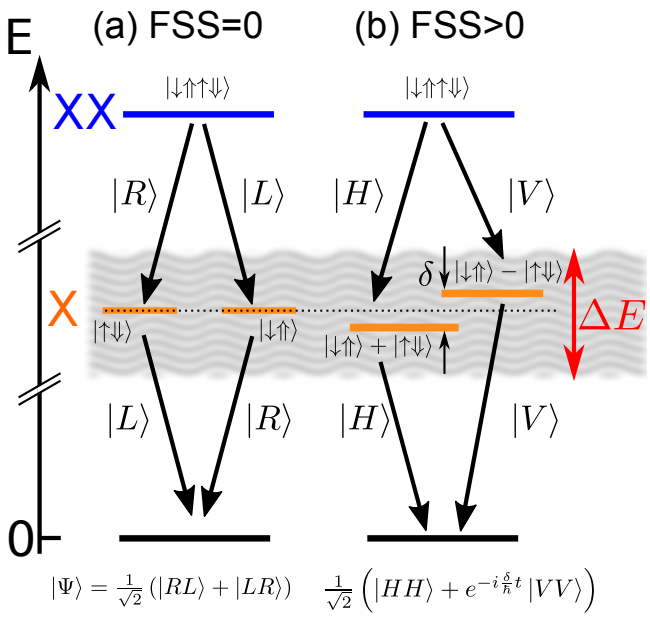

Fig. 1. Representation of the biexciton (XX) exciton (X) emission. (a) In case of zero FSS the X-levels are degenerate and the two decay paths are indistinguishable which creates the entangled photon state $\frac{1}{\sqrt{2}}(|RL\rangle + |LR\rangle)$. (b) For non-zero FSS the X-level is split by δ and the quantum state will precess between these two states. However, with a fast measurement ($\Delta E \geq \delta$) the two X states (in H/V basis) cannot be resolved anymore and removes the which-path information. The wavy gray background indicates the uncertainty introduced through the measurement process.

detection system ($\tau \ll \hbar/\delta$) will render the two decay pathways indistinguishable since the energy uncertainty relation $\Delta E \geq \frac{\hbar}{2\tau}$ does not allow for a precise energy measurement anymore. This point of view is complementary to spectral filtering [41,42] where only states with the same energy are analyzed but at the expense of filtering off many entangled photons. Please note that compared to employing spectral filtering a detection system with a high time resolution does not loose any photons, only each time bin will have a different phase (compare Eq. (1)), as shown by several experiments [7,39] resolving the so-called quantum oscillations. Nevertheless, a finite detector time resolution *always* introduces phase averaging and inevitably reduces the measurable entanglement. In the following, we will quantify this effect of reduced measured entanglement between the excitons in case of finite FSS with a photon detector of finite time resolution. In a quantum state tomography measurement [43] the state described in Eq. (1) is projected on the measurement basis $\langle ij|$, where $\mathrm{i,j} \in \{ H, V, D, A, R, L \}$ with D, A denoting the diagonal and anti-diagonal polarization states, respectively. We define the time evolution of the measured biexciton-exciton pair rate as $n(t, \tau_X) = \frac{N_0}{\tau_X} e^{-t/\tau_X}$ for $t \geq 0$ and $n(t, \tau_X) = 0$ otherwise. Here, t denotes the time after biexciton emission, τ_X the lifetime of the exciton level, and N_0 the number of detected photon pairs. In case of perfect time resolution, we get a time dependent correlation rate in each projection i, j as

$$n_{i,j}(t, \delta, \tau_X) = |\langle ij \,|\, \Psi(t, \delta)\rangle|^2 n(t, \tau_X). \tag{2}$$

The effect of finite time resolution of the detection system is modeled by $g(t, \tau)$, a Gaussian with full width at half maximum of τ. In such circumstances, the detected projections are given by a

Optics EXPRESS

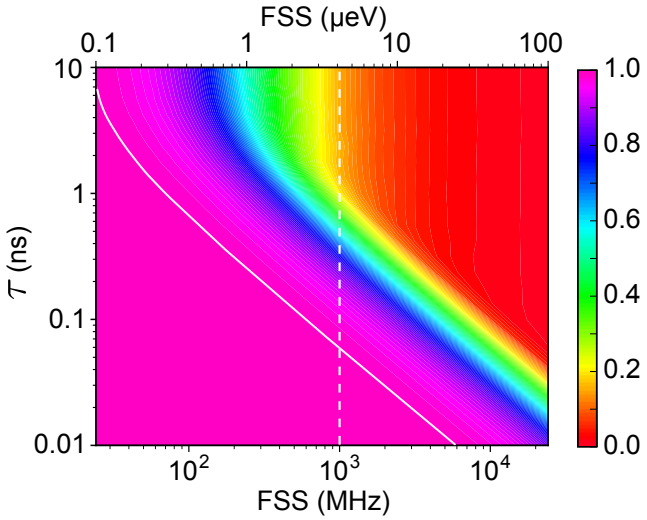

Fig. 2. The measurable entanglement represented as the averaged concurrence $\bar{C}$ as a function of the detector time resolution (τ) and fine-structure splitting (FSS) in case of an exciton lifetime of $\tau_X = 1$ ns. The white dashed line is a guide to the eye for the examples in the text and the white solid line highlights the 0.99 contour line.

convolution of the detection time resolution with Eq. (2) yielding

$$m_{i,j}(t, \delta, \tau, \tau_X) = n_{i,j}(t, \delta, \tau_X) * g(t, \tau). \tag{3}$$

The amount of entanglement which remains in $m_{i,j}(t, \delta, \tau, \tau_X)$ can be quantified by its concurrence C which lies between zero and one [44]. It is one in case the system is fully entangled and zero if there are only classical correlations present. Since the state with finite FSS is evolving in time we define the time averaged concurrence $\bar{C}$ weighted with the amount of detected photons per infinitesimal time bin as

$$\bar{C}(\delta, \tau, \tau_X) := \lim_{T\to\infty} \frac{1}{N_0} \int_{-T}^{T} n(t) C\left(\rho\left(m_{i,j}\right)\right) dt, \tag{4}$$

where $\rho(m_{i,j})$ denotes the density matrix reconstructed from $m_{i,j}(t, \delta, \tau, \tau_X)$. Equation (4) is evaluated numerically [45] for an exciton lifetime of $\tau_X = 1$ ns and the result is presented in Fig. 2. The result indicates that with sufficiently fast detection, perfect entanglement can be reconstructed. With a state of the art detection system based on superconducting nanowires [46] a time resolution of $\tau = 20$ ps is possible without compromising detection efficiency. A FSS of $\delta = 1$ GHz (white dashed line in Fig. 2), yields a measurement of $\bar{C} = 0.999$ very close to unity. With regular avalanche photodiodes of $\tau = 300$ ps this value already reduces to $\bar{C} = 0.77$. Worsening the detection system resolution further to a time resolution of $\tau = 1$ ns yields almost no entanglement. In this latter case, the concurrence significantly reduces to $\bar{C} = 0.19$. However, the latter nanosecond time resolution would be preferred in applications regarding secure communication protocols where accurate timing on picoseconds over kilometers [47] becomes difficult. To solve this issue, we developed a fully optical compensation technique, which reduces the FSS to zero. This allows the application of a photon detection system with less stringent time resolution requirements while maintaining near unity concurrence measurements.

Optics EXPRESS

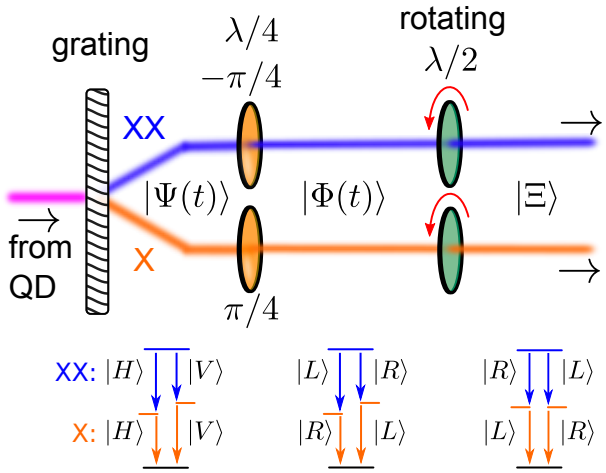

Fig. 3. Proposed optical setup to compensate for a finite FSS. First, a polarization insensitive transmission grating splits the biexciton (XX) from the exciton (X) line. Next, a $\lambda/4$-plate transforms the X and XX photons into the circular basis. Finally, a $\lambda/2$-plate (one for each photon) rotating with an angular frequency of $f = \frac{\delta}{8\pi\hbar}$ compensates for the FSS. The polarization of the photons is indicated underneath the optical path after each waveplate. The length of the arrows is indicative for the photon energy. For convenience possible mirrors have been omitted.

4. Compensating the FSS

In the following, we introduce a method to compensate the FSS, making it possible to employ detection systems with any timing resolution smaller than the QD's photon repetition period such that no overlap between adjacent pulses occur. The evolution of Eq. (1) with finite FSS is unitary due to the time evolving exponential phase factor. Thus, it must be possible [39] to undo this phase evolution by suitable unitary optical components. The main component to achieve complete removal is a rotating $\lambda/2$-waveplate. Such an optical component acts on circularly polarized light as a single sideband frequency shifter [48, 49]. A $\lambda/2$-waveplate spinning with angular frequency ω acting on a photon state can thus be described by the following operator

$$\Lambda_{1/2}(\omega) = \sum_k a^\dagger_{k+\frac{2\omega}{c},L} a_{k,R} + a^\dagger_{k-\frac{2\omega}{c},R} a_{k,L}, \tag{5}$$

where only k-vectors (k) perpendicular to the plane of the waveplate are considered. Here, c denotes the speed of light, and $a_{k,\lambda}$, $a^\dagger_{k,\lambda}$ denote annihilation and creation operators of photons with wavevector of length k and right or left circular polarization $\lambda \in \{R, L\}$, respectively. The action of a rotating $\lambda/2$-waveplate as described by Eq. (5) will up-convert $|R\rangle$ photons by the energy $2\hbar\omega$ and down-convert $|L\rangle$ photons by the same amount. Remarkably, this process can be achieved with unity efficiency. With the help of two $\lambda/4$-waveplates the XX and the X state transform into

$$\begin{aligned} |\Phi(t,\delta)\rangle &= \Lambda_{1/4}(-\pi/4) \otimes \Lambda_{1/4}(\pi/4) \, |\Psi(t,\delta)\rangle \\ &= \frac{1}{\sqrt{2}} \left(|LR\rangle + e^{-i\frac{\delta}{\hbar}t} \, |RL\rangle \right), \end{aligned} \tag{6}$$

where the angles $\pm\pi/4$ are oriented with respect to the horizontal orientation. Now, sending this new state $|\Phi(t,\delta)\rangle$ through a spinning $\lambda/2$-waveplate rotating with angular frequency of $\omega = \frac{\delta}{4\hbar}$

Optics EXPRESS

yields an entangled Bell state

$$\begin{aligned} |\Xi\rangle &= \Lambda_{1/2}\left(\frac{\delta}{4\hbar}\right) \otimes \Lambda_{1/2}\left(\frac{\delta}{4\hbar}\right) |\Phi(t,\delta)\rangle \\ &= \frac{1}{\sqrt{2}}\left(|RL\rangle + |LR\rangle\right), \end{aligned} \tag{7}$$

where the time dependent phase factor has been completely removed. Here, $\Lambda_{1/2}(\omega)$ represents the operator from Eq. (5). For a detailed derivation of Eq. (7) see the Appendix. A possible setup to erase the FSS is depicted in Fig. 3. First, a dispersive element, such as a high efficiency transmission grating, splits the XX line from the X line. Next, the XX (X) photon is sent through a fixed $\lambda/4$ waveplate offset from the horizontal direction by $-\pi/4$ ($\pi/4$). The photon state at this stage is represented by Eq. (6). Finally, letting them both pass through a rotating $\lambda/2$-waveplate with angular frequency $\omega = \frac{\delta}{4\hbar}$ removes the FSS completely. A rotating $\lambda/2$-waveplate can be implemented with electro-optical modulators (EOM) [50, 51]. In this case, the conversion efficiency is only limited by the transmission through the EOM. In fact, owing to the high transparency of EOMs a 95 % conversion efficiency was achieved [52]. Note, in contrast to a rotating $\lambda/2$-waveplate the EOM approach needs twice the angular frequency to obtain the same frequency shift [50]. For example, the RF frequency ($f = \frac{\omega}{\pi} = \frac{\delta}{4\pi\hbar}$) necessary to compensate a FSS of 10 μeV with the EOM approach is 1209 MHz, which is easily achievable with current EOM technology [50] reaching tens of GHz modulation bandwidth. In particular, the frequency shifting based on a rotating waveplate implementation has the advantage of only utilizing two single tone RF signals [50] which can be generated and amplified with off-the-shelf RF equipment. In contrast, the linear ramp approach by Wang et al. [32] can even with costly tens of GHz broadband RF equipment merely approximate a linear voltage ramp as higher harmonics are cut eventually. As our proposed technique is not invasive on the sample containing the QDs it is possible to compensate for the FSS of every QD as long as the EOM's frequency can be tuned to compensate the FSS of the QD under study. This feature renders our approach universally applicable, as simply a different RF frequency needs to be applied to compensate the FSS of a different QD.

5. Conclusions

In summary, we have analyzed the effect of finite FSS and the influence of the detection time resolution on the measurable entanglement from a single QD via the biexciton-exciton cascade. The uncertainty in energy and time in the measurement allows the emitted QD photons to be entangled when a detection system with sufficient timing resolution is employed. However, the precise timing requirement on a picosecond level is hampering the progress in making the entanglement useful for applications and research. We have proposed a universal optical setup to completely remove the FSS based on a rotating $\lambda/2$-plate, which can be implemented with current EOM technology. The proposed technique will allow making the entanglement created from QDs available for many applications like quantum communication, sensing, and imaging.

Appendix

To understand in detail the compensation procedure the typical equation of the entangled state with fine-structure splitting δ, written as

$$|\Psi(t,\delta)\rangle = \frac{1}{\sqrt{2}}\left(|HH\rangle + e^{-i\frac{\delta}{\hbar}t}\,|VV\rangle\right), \tag{8}$$

needs to be rewritten in terms of creation operators $a^{\dagger}_{z,k,\lambda}$ since Eq. (8) is ambiguous about the time ordering of the excitons (biexciton is emitted before the exciton) and their energies.

Optics EXPRESS

The first index of the creation operator z represent the position of the photon perpendicular to waveplate orientation, k the wave vector, and λ the polarization state. For the sake of clarity and taking into account the actual experimental implementation, we only consider photons traveling perpendicular to the waveplate orientation and neglect any vector representation in the following. To capture the photon ordering the emission times of the biexciton $t_{\mathbf{XX}}$ and the exciton t_X are introduced. The time t as in Eq. (8) is defined as $t := t_X - t_{\mathbf{XX}}$. The energies of the excitons are described by their wave vectors $k_{\mathbf{XX}}$ and k_X, respectively. For photons in vacuum the dispersion relation holds

$$E = \hbar\omega = \hbar k c, \tag{9}$$

with c the speed of light. Furthermore, for the sake of clarity the FSS is expressed as $\Delta k = \frac{\delta}{2\hbar c}$. With these definitions at hand we can write the entangled state in Eq. (8) as

$$\begin{aligned}\Psi(z, t_{\mathbf{XX}}, t_X, k_{\mathbf{XX}}, k_X, \Delta k) = \frac{1}{\sqrt{2}} \Big(& a^\dagger_{z-t_{\mathbf{XX}}c, k_{\mathbf{XX}}+\Delta k, H} a^\dagger_{z-t_X c, k_X-\Delta k, H} \\ & + a^\dagger_{z-t_{\mathbf{XX}}c, k_{\mathbf{XX}}-\Delta k, V} a^\dagger_{z-t_X c, k_X+\Delta k, V} \Big)\end{aligned} \tag{10}$$

which can be shown to be equal to Eq. (8)

$$\begin{aligned}\Psi(z, t_{\mathbf{XX}}, t_X, k_{\mathbf{XX}}, k_X, \Delta k) &= \frac{1}{\sqrt{2}} \Big(a^\dagger_{z,k_{\mathbf{XX}},H} e^{i(z\Delta k - t_{\mathbf{XX}} k_{\mathbf{XX}} c - t_{\mathbf{XX}} \Delta k c)} a^\dagger_{z,k_X,H} e^{i(-z\Delta k - t_X k_X c + t_X \Delta k c)} \\ &\quad + a^\dagger_{z,k_{\mathbf{XX}},H} e^{i(-z\Delta k - t_{\mathbf{XX}} k_{\mathbf{XX}} c + t_{\mathbf{XX}} \Delta k c)} a^\dagger_{z,k_X,H} e^{i(z\Delta k - t_X k_X c - t_X \Delta k c)} \Big) \\ &= \frac{1}{\sqrt{2}} \left(a^\dagger_{z,k_{\mathbf{XX}},H} a^\dagger_{z,k_X,H} + e^{-i2\Delta k t c} a^\dagger_{z,k_{\mathbf{XX}},V} a^\dagger_{z,k_X,V} \right),\end{aligned} \tag{11}$$

where we have used the fact that overall phases can be factorized out. Now we are ready to show the compensation procedure. As explained in the manuscript, we first have to transform from H/V basis to R/L by means of two $\lambda/4$ plates. One $\lambda/4$ waveplate, represented by the operator $\Lambda_{1/4}$, will act on the XX and with an angle offset from the horizontal direction of $-\pi/4$ and the other on the X with an offset of $\pi/4$. In this way, horizontal and vertical polarization states are transformed to circular basis necessary for the compatibility with the rotating waveplate frequency shifter. In the following equation the action of the two $\lambda/4$ waveplates upon the quantum state (10) is calculated:

$$\begin{aligned}\Phi(z, t_{\mathbf{XX}}, t_X, k_{\mathbf{XX}}, k_X, \Delta k) &= \Lambda_{1/4}(-\pi/4) \otimes \Lambda_{1/4}(\pi/4) \Psi(z, t_{\mathbf{XX}}, t_X, k_{\mathbf{XX}}, k_X, \Delta k) \\ &= \frac{1}{\sqrt{2}} \Big(a^\dagger_{z,k_{\mathbf{XX}},L} e^{i(z\Delta k - t_{\mathbf{XX}} k_{\mathbf{XX}} c - t_{\mathbf{XX}} \Delta k c)} a^\dagger_{z,k_X,R} e^{i(-z\Delta k - t_X k_X c + t_X \Delta k c)} \\ &\quad + a^\dagger_{z,k_{\mathbf{XX}},R} e^{i(-z\Delta k - t_{\mathbf{XX}} k_{\mathbf{XX}} c + t_{\mathbf{XX}} \Delta k c)} a^\dagger_{z,k_X,L} e^{i(+z\Delta k - t_X k_X c - t_X \Delta k c)} \Big) \\ &= \frac{1}{\sqrt{2}} \left(a^\dagger_{z,k_{\mathbf{XX}},L} a^\dagger_{z,k_X,R} + e^{-i2\Delta k t c} a^\dagger_{z,k_{\mathbf{XX}},R} a^\dagger_{z,k_X,L} \right).\end{aligned} \tag{12}$$

For convenience we can in Eq. (12) omit z and replace $t_{\mathbf{XX}}$ and t_X with t, then the quantum state reads

$$\Phi(t, k_{\mathbf{XX}}, k_X, \Delta k) = \frac{1}{\sqrt{2}} \left(a^\dagger_{k_{\mathbf{XX}},L} a^\dagger_{k_X,R} + e^{-i2\Delta k t c} a^\dagger_{k_{\mathbf{XX}},R} a^\dagger_{k_X,L} \right). \tag{13}$$

Optics EXPRESS

The rotating $\lambda/2$-waveplate, represented by the operator

$$\Lambda_{1/2}(\omega) = \sum_k a^\dagger_{k+\frac{2\omega}{c},L} a_{k,R} + a^\dagger_{k-\frac{2\omega}{c},R} a_{k,L}, \tag{14}$$

where ω represents the angular rotation frequency, will consequently remove the effect of the fine-structure splitting if $\omega = \frac{\delta}{4\hbar}$:

$$\begin{aligned}
\Xi(k_{\mathbf{X}}, k_X) &= \Lambda_{1/2}\left(\frac{\delta}{4\hbar}\right) \otimes \Lambda_{1/2}\left(\frac{\delta}{4\hbar}\right) \Phi(z, t_{\mathbf{X}}, t_X, k_{\mathbf{X}}, k_X, \Delta k) \\
&= \Lambda_{1/2}\left(\frac{\delta}{4\hbar}\right) \otimes \Lambda_{1/2}\left(\frac{\delta}{4\hbar}\right) \frac{1}{\sqrt{2}} \left(a^\dagger_{z-t_{\mathbf{X}}c, k_{\mathbf{X}}+\Delta k, L} a^\dagger_{z-t_X c, k_X-\Delta k, R}\right. \\
&\quad \left. + a^\dagger_{z-t_{\mathbf{X}}c, k_{\mathbf{X}}-\Delta k, R} a^\dagger_{z-t_X c, k_X+\Delta k, L}\right) \\
&= \frac{1}{\sqrt{2}} \left(a^\dagger_{z-t_{\mathbf{X}}c, k_{\mathbf{X}}, R} a^\dagger_{z-t_X c, k_X, L} + a^\dagger_{z-t_{\mathbf{X}}c, k_{\mathbf{X}}, L} a^\dagger_{z-t_X c, k_X, R}\right) \\
&= \frac{1}{\sqrt{2}} \left(a^\dagger_{z, k_{\mathbf{X}}, R} a^\dagger_{z, k_X, L} e^{-ik_{\mathbf{X}} t_{XX} c - ik_X t_X c} + a^\dagger_{z, k_{\mathbf{X}}, L} a^\dagger_{z, k_X, R} e^{-ik_{\mathbf{X}} t_{XX} c - ik_X t_X c}\right) \\
&= \frac{1}{\sqrt{2}} \left(a^\dagger_{z, k_{\mathbf{X}}, R} a^\dagger_{z, k_X, L} + a^\dagger_{z, k_{\mathbf{X}}, L} a^\dagger_{z, k_X, R}\right).
\end{aligned} \tag{15}$$

The last line in Eq. (15) is a fully entangled state without FSS in circular basis. Therefore, it is not yet precisely the starting state as described in Eq. (8) without the exponential phase term. But with the addition of two $\lambda/4$-waveplates the state can be translated in to H/V basis and is then equivalent to our initial state described in Eq. (8) without FSS:

$$\Lambda_{1/4}(-\pi/4) \otimes \Lambda_{1/4}(\pi/4)\, \Xi(k_{\mathbf{X}}, k_X) = \frac{1}{\sqrt{2}} \left(a^\dagger_{z, k_{\mathbf{X}}, H} a^\dagger_{z, k_X, H} + a^\dagger_{z, k_{\mathbf{X}}, V} a^\dagger_{z, k_X, V}\right). \tag{16}$$

Funding

Swiss National Science Foundation for the support through their Early PostDoc Mobility Program (P2EZP2_165240) for A. Fognini, Industry Canada and NSERC (RGPIN-2016-04152).

Acknowledgment

The authors thank Iman Esmaeil Zadeh for discussing the topic.

References

1. O. Benson, C. Santori, M. Pelton, and Y. Yamamoto, "Regulated and entangled photons from a single quantum dot," Phys. Rev. Lett. **84**, 2513–2516 (2000).
2. C. L. Salter, R. M. Stevenson, I. Farrer, C. A. Nicoll, D. A. Ritchie, and A. J. Shields, "An entangled-light-emitting diode," Nature **465**, 594–597 (2010).
3. R. Hafenbrak, S. M. Ulrich, P. Michler, L. Wang, A. Rastelli, and O. G. Schmidt, "Triggered polarization-entangled photon pairs from a single quantum dot up to 30 K," New J. Phys. **9**, 315 (2007).
4. E. Moreau, I. Robert, L. Manin, V. Thierry-Mieg, J. M. Gérard, and I. Abram, "Quantum cascade of photons in semiconductor quantum dots," Phys. Rev. Lett. **87**, 183601 (2001).
5. R. Seguin, A. Schliwa, S. Rodt, K. Pötschke, U. W. Pohl, and D. Bimberg, "Size-dependent fine-structure splitting in self-organized InAs/GaAs quantum dots," Phys. Rev. Lett. **95**, 257402 (2005).
6. R. Singh and G. Bester, "Nanowire quantum dots as an ideal source of entangled photon pairs," Phys. Rev. Lett. **103**, 063601 (2009).
7. T. Huber, A. Predojević, M. Khoshnegar, D. Dalacu, P. J. Poole, H. Majedi, and G. Weihs, "Polarization entangled photons from quantum dots embedded in nanowires," Nano Lett. **14**, 7107–7114 (2014).
8. S. Seidl, M. Kroner, A. Högele, K. Karrai, R. J. Warburton, A. Badolato, and P. M. Petroff, "Effect of uniaxial stress on excitons in a self-assembled quantum dot," Appl. Phys. Lett. **88**, 203113 (2006).

Optics EXPRESS

9. G. Bester, S. Nair, and A. Zunger, "Pseudopotential calculation of the excitonic fine structure of million-atom self-assembled $In_{1-x}Ga_xAs$/GaAs quantum dots," Phys. Rev. B **67**, 161306 (2003).
10. M. Bayer, G. Ortner, O. Stern, A. Kuther, A. A. Gorbunov, A. Forchel, P. Hawrylak, S. Fafard, K. Hinzer, T. L. Reinecke, S. N. Walck, J. P. Reithmaier, F. Klopf, and F. Schäfer, "Fine structure of neutral and charged excitons in self-assembled In(Ga)As/(Al)GaAs quantum dots," Phys. Rev. B **65**, 195315 (2002).
11. T. M. Stace, G. J. Milburn, and C. H. W. Barnes, "Entangled two-photon source using biexciton emission of an asymmetric quantum dot in a cavity," Phys. Rev. B **67**, 085317 (2003).
12. R. M. Stevenson, R. J. Young, P. Atkinson, K. Cooper, D. A. Ritchie, and A. J. Shields, "A semiconductor source of triggered entangled photon pairs," Nature **439**, 179–182 (2006).
13. T. Kuroda, T. Mano, N. Ha, H. Nakajima, H. Kumano, B. Urbaszek, M. Jo, M. Abbarchi, Y. Sakuma, K. Sakoda, I. Suemune, X. Marie, and T. Amand, "Symmetric quantum dots as efficient sources of highly entangled photons: Violation of Bell′s inequality without spectral and temporal filtering," Phys. Rev. B **88**, 041306 (2013).
14. G. Juska, V. Dimastrodonato, L. O. Mereni, A. Gocalinska, and E. Pelucchi, "Towards quantum-dot arrays of entangled photon emitters," Nat. Photonics **7**, 527–531 (2013).
15. M. A. M. Versteegh, M. E. Reimer, K. D. Jöns, D. Dalacu, P. J. Poole, A. Gulinatti, A. Giudice, and V. Zwiller, "Observation of strongly entangled photon pairs from a nanowire quantum dot," Nat. Commun. **5**, 5298 (2014).
16. R. Trotta, J. Martín-Sánchez, I. Daruka, C. Ortix, and A. Rastelli, "Energy-tunable sources of entangled photons: A viable concept for solid-state-based quantum relays," Phys. Rev. Lett. **114**, 150502 (2015).
17. K. Kowalik, O. Krebs, A. Lemaître, S. Laurent, P. Senellart, P. Voisin, and J. A. Gaj, "Influence of an in-plane electric field on exciton fine structure in InAs – GaAs self-assembled quantum dots," Appl. Phys. Lett. **86**, 041907 (2005).
18. A. Muller, W. Fang, J. Lawall, and G. S. Solomon, "Creating polarization-entangled photon pairs from a semiconductor quantum dot using the optical stark effect," Phys. Rev. Lett. **103**, 217402 (2009).
19. W. Langbein, P. Borri, U. Woggon, V. Stavarache, D. Reuter, and A. D. Wieck, "Control of fine-structure splitting and biexciton binding in $In_xGa_{1-x}As$ quantum dots by annealing," Phys. Rev. B **69**, 161301 (2004).
20. R. Trotta, E. Zallo, C. Ortix, P. Atkinson, J. D. Plumhof, J. van den Brink, A. Rastelli, and O. G. Schmidt, "Universal recovery of the energy-level degeneracy of bright excitons in InGaAs quantum dots without a structure symmetry," Phys. Rev. Lett. **109**, 147401 (2012).
21. N. Somaschi, V. Giesz, L. De Santis, J. C. Loredo, M. P. Almeida, G. Hornecker, S. L. Portalupi, T. Grange, C. Antón, J. Demory, C. Gómez, I. Sagnes, N. D. Lanzillotti-Kimura, A. Lemaítre, A. Auffeves, A. G. White, L. Lanco, and P. Senellart, "Near-optimal single-photon sources in the solid state," Nat. Photonics **10**, 340–345 (2016).
22. P. E. Kremer, A. C. Dada, P. Kumar, Y. Ma, S. Kumar, E. Clarke, and B. D. Gerardot, "Strain-tunable quantum dot embedded in a nanowire antenna," Phys. Rev. B **90**, 201408 (2014).
23. M. Munsch, N. S. Malik, E. Dupuy, A. Delga, J. Bleuse, J.-M. Gérard, J. Claudon, N. Gregersen, and J. Mørk, "Dielectric GaAs antenna ensuring an efficient broadband coupling between an InAs quantum dot and a gaussian optical beam," Phys. Rev. Lett. **110**, 177402 (2013).
24. J. Claudon, J. Bleuse, N. S. Malik, M. Bazin, P. Jaffrennou, N. Gregersen, C. Sauvan, P. Lalanne, and J.-M. Gerard, "A highly efficient single-photon source based on a quantum dot in a photonic nanowire," Nat. Photonics **4**, 174–177 (2010).
25. E. Moreau, I. Robert, J. M. Gérard, I. Abram, L. Manin, and V. Thierry-Mieg, "Single-mode solid-state single photon source based on isolated quantum dots in pillar microcavities," Appl. Phys. Lett. **79**, 2865–2867 (2001).
26. M. Pelton, C. Santori, J. Vučković, B. Zhang, G. S. Solomon, J. Plant, and Y. Yamamoto, "Efficient source of single photons: A single quantum dot in a micropost microcavity," Phys. Rev. Lett. **89**, 233602 (2002).
27. S. Unsleber, Y.-M. He, S. Gerhardt, S. Maier, C.-Y. Lu, J.-W. Pan, N. Gregersen, M. Kamp, C. Schneider, and S. Höfling, "Highly indistinguishable on-demand resonance fluorescence photons from a deterministic quantum dot micropillar device with 74 % extraction efficiency," Opt. Express **24**, 8539–8546 (2016).
28. O. Gazzano, S. Michaelis de Vasconcellos, C. Arnold, A. Nowak, E. Galopin, I. Sagnes, L. Lanco, A. Lemaître, and P. Senellart, "Bright solid-state sources of indistinguishable single photons," Nat. Commun. **4**, 1425 (2013).
29. W. Barnes, G. Björk, J. Gérard, P. Jonsson, J. Wasey, P. Worthing, and V. Zwiller, "Solid-state single photon sources: light collection strategies," Eur. Phys. J. D **18**, 197–210 (2002).
30. G. Bulgarini, M. E. Reimer, M. Bouwes Bavinck, K. D. Jöns, D. Dalacu, P. J. Poole, E. P. A. M. Bakkers, and V. Zwiller, "Nanowire waveguides launching single photons in a gaussian mode for ideal fiber coupling," Nano Lett. **14**, 4102–4106 (2014).
31. H. Wang, Y. He, Y.-H. Li, Z.-E. Su, B. Li, H.-L. Huang, X. Ding, M.-C. Chen, C. Liu, J. Qin, J.-P. Li, Y.-M. He, C. Schneider, M. Kamp, C.-Z. Peng, S. Höfling, C.-Y. Lu, and J.-W. Pan, "High-efficiency multiphoton boson sampling," Nat. Photonics **11**, 361–365 (2017).
32. X.-B. Wang, C.-X. Yang, and Y.-B. Liu, "On-demand entanglement source with polarization-dependent frequency shift," Appl. Phys. Lett. **96**, 201103 (2010).
33. N. S. Jones and T. M. Stace, "Photon frequency-mode matching using acousto-optic frequency beam splitters," Phys. Rev. A **73**, 033813 (2006).
34. W. A. Coish and J. M. Gambetta, "Entangled photons on demand: Erasing which-path information with sidebands," Phys. Rev. B **80**, 241303 (2009).
35. M. Metcalfe, S. M. Carr, A. Muller, G. S. Solomon, and J. Lawall, "Resolved sideband emission of InAs/GaAs quantum dots strained by surface acoustic waves," Phys. Rev. Lett. **105**, 037401 (2010).

Optics EXPRESS

36. Z.-Q. Zhou, C.-F. Li, G. Chen, J.-S. Tang, Y. Zou, M. Gong, and G.-C. Guo, "Phase compensation enhancement of photon pair entanglement generated from biexciton decay in quantum dots," Phys. Rev. A **81**, 064302 (2010).
37. A. J. Hudson, R. M. Stevenson, A. J. Bennett, R. J. Young, C. A. Nicoll, P. Atkinson, K. Cooper, D. A. Ritchie, and A. J. Shields, "Coherence of an entangled exciton-photon state," Phys. Rev. Lett. **99**, 266802 (2007).
38. E. Poem, Y. Kodriano, C. Tradonsky, N. H. Lindner, B. D. Gerardot, P. M. Petroff, and D. Gershoni, "Accessing the dark exciton with light," Nat. Phys. **6**, 993–997 (2010).
39. R. M. Stevenson, A. J. Hudson, A. J. Bennett, R. J. Young, C. A. Nicoll, D. A. Ritchie, and A. J. Shields, "Evolution of entanglement between distinguishable light states," Phys. Rev. Lett. **101**, 170501 (2008).
40. C. Santori, D. Fattal, M. Pelton, G. S. Solomon, and Y. Yamamoto, "Polarization-correlated photon pairs from a single quantum dot," Phys. Rev. B **66**, 045308 (2002).
41. N. Akopian, N. H. Lindner, E. Poem, Y. Berlatzky, J. Avron, D. Gershoni, B. D. Gerardot, and P. M. Petroff, "Entangled photon pairs from semiconductor quantum dots," Phys. Rev. Lett. **96**, 130501 (2006).
42. N. Akopian, N. H. Lindner, E. Poem, Y. Berlatzky, J. Avron, D. Gershoni, B. D. Gerardot, and P. M. Petroff, "Correlated and entangled pairs of single photons from semiconductor quantum dots," J. Appl. Phys. **101**, 081712 (2007).
43. D. F. V. James, P. G. Kwiat, W. J. Munro, and A. G. White, "Measurement of qubits," Phys. Rev. A **64**, 052312 (2001).
44. W. K. Wootters, "Entanglement of formation of an arbitrary state of two qubits," Phys. Rev. Lett. **80**, 2245–2248 (1998).
45. T. Fokkens, A. Fognini, and V. Zwiller, "Quantum tomography on optical two qubit states," (2016-2017). Tomography Library, available at https://github.com/afognini/Tomography.
46. I. Esmaeil Zadeh, J. W. N. Los, R. B. M. Gourgues, V. Steinmetz, G. Bulgarini, S. M. Dobrovolskiy, V. Zwiller, and S. N. Dorenbos, "Single-photon detectors combining high efficiency, high detection rates, and ultra-high timing resolution," APL Photonics **2**, 111301 (2017).
47. R. Ursin, F. Tiefenbacher, T. Schmitt-Manderbach, H. Weier, T. Scheidl, M. Lindenthal, B. Blauensteiner, T. Jennewein, J. Perdigues, P. Trojek, B. Omer, M. Furst, M. Meyenburg, J. Rarity, Z. Sodnik, C. Barbieri, H. Weinfurter, and A. Zeilinger, "Entanglement-based quantum communication over 144 km," Nat. Phys. **3**, 481–486 (2007).
48. P. Page and H. Pursey, "Tunable single sideband electro-optic ring modulator," Opto-electronics **2**, 1–4 (1970).
49. G. H. Smith, D. Novak, and Z. Ahmed, "Technique for optical ssb generation to overcome dispersion penalties in fibre-radio systems," Electron. Lett. **33**, 74–75 (1997).
50. C. Qin, H. Lu, B. Ercan, S. Li, and S. J. B. Yoo, "Single-tone optical frequency shifting and nonmagnetic optical isolation by electro-optical emulation of a rotating half-wave plate in a traveling-wave lithium niobate waveguide," IEEE Photon. J. **9**, 1–13 (2017).
51. P. Gangding, H. Shangyuan, and L. Zonggi, "Application of electro-optic frequency shifters in heterodyne interferometric systems," Electron. Lett. **22**, 1215–1216 (1986).
52. R. Noe and D. A. Smith, "Integrated-optic rotating waveplate frequency shifter," Electron. Lett. **24**, 1348–1349 (1988).